

Analysis of acoustic wave fronts in the atmosphere to profile the temperature and wind with a radio acoustic sounding system

K. Takahashi, Y. Masuda, and N. Matuura
Radio Research Laboratory, 4-2-1 Nukuikita, Koganei, Tokyo 184, Japan

S. Kato, S. Fukao, T. Tsuda, and T. Sato
Radio Atmospheric Science Center, Kyoto University, Uji, Kyoto 611, Japan

(Received 18 March 1987; accepted for publication 7 June 1988)

Differential equations were introduced to analyze the acoustic wave fronts in the atmosphere. The wave fronts were found to make an ellipsoid whose major principal axis tilts at an angle of about 45° to the leeward. Utilizing this result, a radio acoustic sounding system (RASS) was used to measure the temperature and wind profiles to heights of over 23 km even under strong wind conditions. The profiles agree with those obtained from a radiosonde and a Doppler radar. The discrepancies are only about 0.5 °C in the air temperature and 1 m/s in the wind speed. The experiments show that the analytical result of the acoustic wave fronts is effective not only in the troposphere but also in the stratosphere. The analysis also shows quantitatively that acoustic waves propagate over the horizon to leeward.

PACS numbers: 43.28.Gq, 43.28.Vd

INTRODUCTION

A radio acoustic sounding system (RASS), comprising a Doppler radar and an acoustic transmitter, has been developed to profile the air temperature from the Doppler frequency of radar echoes partially reflected under Bragg conditions on the acoustic wave fronts, by using the dependence of acoustic speed on temperature. With a conventional RASS, the air-temperature profiles have only been measured up to heights of 3.2 km under light wind conditions,¹ because the acoustic wave front has been regarded as a spherical surface, and it is difficult to receive the echo from the surface drifting with the wind.

To measure the temperature and wind profiles up to heights of 20 km or more, even under strong wind conditions, the acoustic wave front in the atmosphere is analyzed by introducing the differential equations. These differential equations are solved by considering the refraction and bending of an acoustic wave ray caused by both the temperature gradient and the wind shear. By transmitting the radio wave from the radar so that the radar beam can intersect the acoustic wave front perpendicularly, the predicted profiles have been measured.

The analysis of the acoustic wave front in the atmosphere also quantitatively explains acoustic wave propagation for extraordinarily long distances over the horizon. This has been a riddle since the 16th century.

I. ACOUSTIC WAVE FRONTS IN THE ATMOSPHERE

In most cases where the vertical component of wind velocity can be ignored, the equations of motion of an acoustic wave front in the atmosphere are derived as follows (refer to Fig. 1):

$$\dot{x} = s \sin \theta \cos \varphi + v, \quad (1)$$

$$\dot{y} = s \sin \varphi, \quad (2)$$

$$\dot{z} = s \cos \theta \cos \varphi, \quad (3)$$

where \dot{x} , \dot{y} , and \dot{z} are the time differentials of variables x , y , and z . The x axis is parallel to the wind velocity, the y axis is vertical, and the x , y , and z axes complete a right-handed rectangular coordinate system. Here, θ , φ are the polar angles, s is the acoustic speed, and v is the wind speed.

Integrating Eqs. (1)–(3) with respect to time t and eliminating θ and φ , we get the equation expressing the acoustic wave front.

Strictly speaking, the speeds s and v are functions of time t and position $P(x,y,z)$. However, they will be considered to

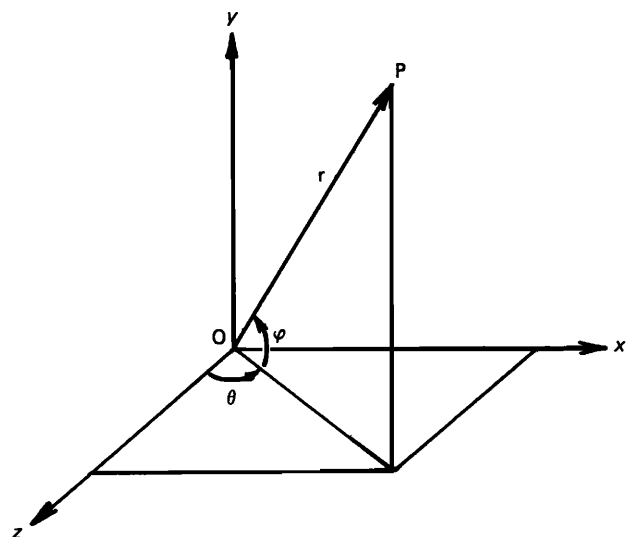


FIG. 1. Coordinate system of equations. The x axis is parallel to the wind velocity, the y axis is vertical, and r , θ , and φ are elements of the polar coordinate.

be average values during the measurement time δt . Then, during δt , according to the definition of the x axis, v can be dealt with as a function solely of y . The speed s is a function of the air temperature T , which is usually regarded as constant on a horizontal plane in the same way that the wind

speed v is regarded as constant. Thus the speed s can also be dealt with as a function solely of y during δt .

Deriving higher-order differentials of Eqs. (1)–(3) and substituting them into the Taylor expansions of x , y , and z , we get the following equations:

$$x = v_0 t + s_0 t \left[\sin \theta_0 \cos \varphi_0 - \sin \theta_0 \sin \varphi_0 \cos \varphi_0 \tau + \frac{1}{2} (1 + \sin^2 \theta_0) \sin \varphi_0 \omega + \frac{1}{2} \cos \theta_0 \cos \varphi_0 \sigma + \frac{1}{3} \sin \theta_0 (2 \sin^2 \varphi_0 - \cos^2 \varphi_0) \cos \varphi_0 \tau^2 + \frac{1}{6} (1 + 3 \sin^2 \theta_0) \cos(2\varphi_0) \tau \omega - \frac{1}{6} (1 + \sin^2 \theta_0) \sin \theta_0 \cos \varphi_0 \omega^2 + \frac{1}{6} \cos \theta_0 \sin \varphi_0 (-2 \cos \varphi_0 \tau + \sin \theta_0 \omega) \sigma - \frac{1}{6} \sin \theta_0 \cos \varphi_0 \sigma^2 + \frac{1}{6} \cos \theta_0 \cos \varphi_0 \ddot{\theta} t^2 + \dots \right], \quad (4)$$

$$y = s_0 t \left[\sin \varphi_0 + \frac{1}{2} \cos(2\varphi_0) \tau - \frac{1}{2} \sin \theta_0 \cos \varphi_0 \omega + \frac{1}{6} (\sin^2 \varphi_0 - 5 \cos^2 \varphi_0) \sin \varphi_0 \tau^2 + \frac{2}{3} \sin \theta_0 \sin(2\varphi_0) \tau \omega - \frac{1}{3} \sin^2 \theta_0 \sin \varphi_0 \omega^2 - \frac{1}{6} \cos \theta_0 \cos \varphi_0 \omega \sigma + \dots \right], \quad (5)$$

$$z = s_0 t \left\{ \cos \theta_0 \left[\cos \varphi_0 - \frac{1}{2} \sin(2\varphi_0) \tau + \frac{1}{2} \sin \theta_0 \sin \varphi_0 \omega + \left(\frac{2}{3} \sin^2 \varphi_0 - \frac{1}{3} \cos^2 \varphi_0 \right) \cos \varphi_0 \tau^2 + \frac{1}{2} \sin \theta_0 \cos(2\varphi_0) \tau \omega - \frac{1}{6} \sin^2 \theta_0 \cos \varphi_0 \omega^2 + \frac{1}{6} \cos \theta_0 \sin \varphi_0 \omega \sigma - \frac{1}{6} \cos \varphi_0 \sigma^2 \right] + \sin \theta_0 \left[-\frac{1}{2} \cos \varphi_0 \sigma + \frac{1}{3} \sin(2\varphi_0) \tau \sigma - \frac{1}{3} \sin \theta_0 \sin \varphi_0 \omega \sigma - \frac{1}{6} \cos \varphi_0 \ddot{\theta} t^2 \right] + \dots \right\}, \quad (6)$$

where

$$s \equiv s_0 - s'y, \quad (7)$$

$$v \equiv v_0 + v'y, \quad (8)$$

s_0 is the acoustic speed on the plane of $y = 0$, v_0 is the wind speed on the plane of $y = 0$,

$$s' \equiv -\frac{\partial s}{\partial y} \quad (\approx 0.004 \text{ s}^{-1} \text{ in the standard troposphere}), \quad (9)$$

$$v' \equiv \frac{\partial v}{\partial y}, \quad (10)$$

$$\tau \equiv s't, \quad (11)$$

$$\omega \equiv v't, \quad (12)$$

$$\sigma \equiv \dot{\theta} t,$$

$$\begin{aligned} \dot{\varphi} &= (s' \cos \varphi - v' \sin \theta \cos^2 \varphi) - v' \sin \theta \sin^2 \varphi \\ &= s' \cos \varphi - v' \sin \theta, \end{aligned} \quad (13)$$

$$x = y = z = 0, \quad \theta = \theta_0, \quad \text{and} \quad \varphi = \varphi_0 \quad \text{at} \quad t = 0.$$

Equation (13) expresses the bending of an acoustic ray in a plane of constant θ . The term $(s' \cos \varphi - v' \sin \theta \cos^2 \varphi)$ expresses the bending caused by the refraction, i.e., wave front rotation through Snell's law (refer to Appendix A). The term $-v' \sin \theta \sin^2 \varphi$ expresses the bending caused directly by the wind shear (refer to Appendix B).

The variables v_0 , v' , s_0 , and s' are all functions of time t and position P . During the measurement time δt , they are regarded as average values in the same way as v and s .

The differential equation (13) is easily solved where s' , v' , and θ are constant, and expressed as follows:

$$\tan \frac{\varphi}{2} = \tan \frac{\varphi_0}{2} - \frac{\sqrt{v'^2 - s'^2}}{v' + s'} \tan \frac{\sqrt{v'^2 - s'^2}}{2} t,$$

where $0 < s' < v'$ and $\theta = \pi/2$. For $\varphi = -\varphi_0$, the value t is expressed as follows:

$$t_\varphi = \frac{2}{\sqrt{v'^2 - s'^2}} \tan^{-1} \left(\frac{2(v' + s')}{\sqrt{v'^2 - s'^2}} \tan \frac{\varphi_0}{2} \right).$$

The acoustic waves can propagate over the horizon under the condition of the following approximation:

$$2\varphi_0 > (s + v)t_\varphi/a,$$

where a is the earth radius.

Substituting the typical values at middle latitudes into the above formulas, we get

$$\varphi_0 > 0.0183 \tan^{-1} [6 \tan(\varphi_0/2)],$$

where

$$\begin{aligned} s' &= 0.004 \text{ s}^{-1}, \\ v' &= 0.005 \text{ s}^{-1}, \\ s + v &= 350 \text{ m/s}, \\ a &= 6.37 \times 10^6 \text{ m}. \end{aligned}$$

The above inequality is valid for $0 < \varphi_0 < \pi/2$. Namely, Eq. (13) shows that acoustic waves usually propagate over the horizon to leeward.

In the ordinary atmosphere at a height of 10 km or below, the absolute values of τ and ω are observed to be less

than 0.1. Neglecting the second- and higher-order terms of τ and ω in Eqs. (4)–(6), and removing σ , θ_0 , and φ_0 from these equations, we get the equation that expresses an ellipsoid whose principal axis tilts at an angle of 45° to the wind velocity as follows:

$$\mathcal{X}^2 + \mathcal{Y}^2 + \mathcal{Z}^2 + \tau\mathcal{Y} - \omega\mathcal{X}\mathcal{Y} = 1, \quad (14)$$

where

$$\mathcal{X} = (x - v_0 t) / s_0 t, \quad (15)$$

$$\mathcal{Y} = y / s_0 t, \quad (16)$$

$$\mathcal{Z} = z / s_0 t. \quad (17)$$

Equation (14) indicates that the acoustic wave front expressed by (1)–(3) is spreading as an ellipsoidal surface. Figure 2 shows the elliptical intersection line of the surface with a plane of $z = 0$ in the case where the second- and higher-order terms are also taken into consideration. Equation (14) also indicates that the acoustic wave front is approximated by a sphere with an underground center where there is a negative temperature gradient and no wind shear, i.e., where $s' > 0$ and $v' = 0$.

Partially differentiating Eq. (14) with respect to x , y , and z to obtain an equation of a normal to the ellipsoidal surface and substituting the values of the origin into the equation, we get

$$\frac{x}{x - v_0 t - \omega y / 2} = \frac{y}{y + \tau s_0 t / 2 - \omega(x - v_0 t) / 2} = \frac{z}{z}. \quad (18)$$

This equation represents the condition where a normal of Eq. (14) passes through the origin $O(0,0,0)$. This means that a radio wave emitted from the origin O is partially reflected at the position (P) and received back at the origin. Here, P must simultaneously satisfy Eqs. (14) and (18).

In general, the curve of second degree, which passes through a point O inside an ellipsoid and intersects the ellipsoid at two positions P where two lines OP meet the ellipsoid at right angles, is a hyperbola. Figure 2 shows this relation-

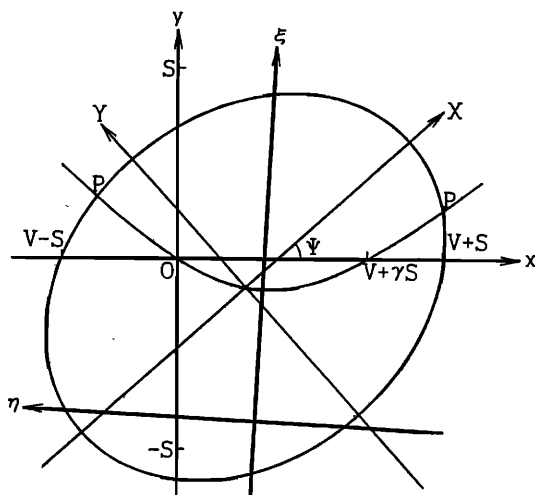


FIG. 2. Acoustic wave front ellipse, and hyperbola that passes through the origin O , and reflection positions P_1 and P_2 . Here, the X , Y axes are the principal axes of the ellipse, the ξ , η axes are the principal axes of the hyperbola, $V = v_0 t$, $S = s_0 t$, and $\gamma = s' / v'$.

ship for $z = 0$, where the X , Y axes show the principal axes of the ellipse and the ξ , η axes show the principal axes of the rectangular hyperbola that passes through O , the origin of the x , y coordinates, and intersects the ellipse at the positions P .

When $z \neq 0$ and $v' \neq 0$, the following values are obtained from Eqs. (14) and (18):

$$x = [v_0 + (s' / v') s_0] t,$$

$$y = -2v_0 / v',$$

$$z = \pm \sqrt{1 - (s' / v')^2 - (2v_0 / \omega s_0)^2} s_0 t.$$

In the normal atmosphere, the value of y in the above equation is negative, and the value of z is imaginary at least in the lower atmosphere. In other words, when $z \neq 0$ and $v' \neq 0$, the elevation angle of the reflection point viewed from the acoustic source is usually negative or there is no reflection point. Therefore, only the case where $z = 0$ and $v' \neq 0$ will be considered.

Considering not only the first-order terms but also the second-order terms of τ and ω in Eqs. (4) and (5), substituting $\pi/2$ for θ_0 , and eliminating σ and most of φ_0 from the resultants, we get the two-dimensional equation as follows:

$$(1 - \frac{1}{2}\omega^2)\mathcal{X}^2 + (1 + \frac{1}{2}\omega^2)\mathcal{Y}^2 - \omega\mathcal{X}\mathcal{Y} - \frac{1}{2}\tau\omega\mathcal{X} + \tau\mathcal{Y} = 1 + \frac{1}{2}\tau^2 - \frac{1}{2}\cos(2\varphi_0)\cos\varphi_0\tau\omega. \quad (19)$$

To eliminate φ_0 from Eq. (19), we can adopt the following approximation, because only high-elevation beams are used:

$$\begin{aligned} \frac{1}{2}\cos(2\varphi_0)\cos\varphi_0 &= 0.90804\cos\varphi_0 - 1.31616\cos\varphi_0\sin\varphi_0 + \epsilon, \\ |\epsilon| < 0.0192, \quad \text{where } 26^\circ.3 < \varphi_0 < 153^\circ.7. \end{aligned} \quad (20)$$

Substituting Eq. (20) into Eq. (19) and using Eqs. (4), (5), (15), and (16), whose third- and higher-order terms of τ and ω are neglected, we get

$$(1 - \frac{1}{2}\omega^2)\mathcal{X}^2 + (1 + \frac{1}{2}\omega^2)\mathcal{Y}^2 - (1 + 1.31616\tau)\omega\mathcal{X}\mathcal{Y} + 0.57471\tau\omega\mathcal{X} + \tau\mathcal{Y} = 1 + \frac{1}{2}\tau^2. \quad (21)$$

Equation (21) shows that the shape of the wave front in the $z = 0$ plane is approximately an ellipse whose principal axis X tilts to the wind velocity at an angle Ψ of about 45° , which is derived from Eq. (21) as follows:

$$\begin{aligned} \tan(2\Psi) &= \frac{-(1 + 1.31616\tau)\omega}{(1 - \frac{1}{2}\omega^2) - (1 + \frac{1}{2}\omega^2)} \\ &= 2.4(1 + 1.31616\tau) / \omega. \end{aligned} \quad (22)$$

To get a numerical example other than 45° , substituting the relatively large value $\omega = 0.01t$ and the mean value $\tau = 0.004t$ into (22), we get

$$\begin{aligned} \tan(2\Psi) &= 240(1 + 0.00526t) / t, \\ \Psi &= 44^\circ, \quad \text{where } t = 10 \text{ s.} \end{aligned}$$

This numerical calculation shows that the error in the wave front position from using the approximation equation (21), in which the higher-order terms were neglected, is less than 0.5% in the ordinary lower atmosphere where $30^\circ < \varphi_0 < 150^\circ$.

TABLE I. RASS parameters.

| | Monostatic pulse-Doppler radar | Acoustic transmitter |
|------------------|--------------------------------|-----------------------------------|
| Frequency | 46.5 MHz | 70-120 Hz |
| Radiated power | 1 MW (peak) | 600 W |
| Antenna | Array of 475 crossed Yagis | Hyperbolic horn of 72-cm diameter |
| Antenna gain | 33 dB | 10 dB |
| Beamwidth | 3°.6 | 90° |
| Pulse width | 2 μs | 0.5-1 s |
| Pulse repetition | 2400 pulses per second | 8-16 pulses per 15-31 s |

II. RASS EXPERIMENTS

In Sec. I, it was shown that radar will receive the echoes from positions *P* on the acoustic wave fronts (RASS echoes), where both a radar and an acoustic transmitter are placed at *O* in Fig. 2. In practice, it is impossible to place a radar and an acoustic transmitter at the same point, but it is easy to deduce the relation between the radar beam direction perpendicular to the acoustic wave front and the separation of the radar and the acoustic transmitter. This analytical result has been examined with the authors' RASS, and is confirmed to be valid up to the heights of 23 km by receiving the RASS echoes.

The RASS consists of a megawatt pulse-Doppler radar (the MU radar) developed by Fukao *et al.*² and a 600-W acoustic transmitter developed by Masuda. The parameters of the RASS are shown in Table I.

In the experiments, RASS echoes were always received from just the limited areas that contained *P*s whose range and direction were equal to the values calculated by the method in Sec. I. In Sec. III, the example of the RASS echo profile is given, and the temperature profile is compared with that obtained with a radiosonde. The method for deducing temperature and wind profiles from a RASS echo profile is also shown in the following section.

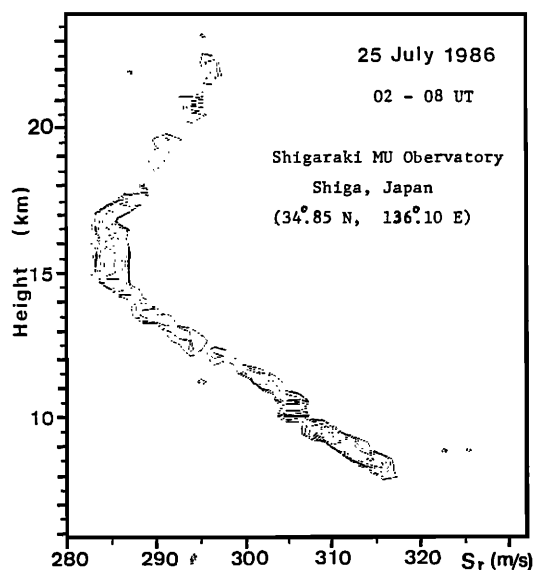


FIG. 3. RASS echo power density spectra in the coordinate system of height versus Doppler velocity *s_r* of acoustic wave fronts.

III. DERIVATION OF TEMPERATURE AND WIND PROFILES

In general, the acoustic speed in the atmosphere is expressed as follows:

$$s = 20.0463T^{1/2} \text{ (m/s)}, \tag{23}$$

where *T* is the absolute air temperature (K). Therefore, *T* is calculated by substituting the speed (Doppler velocity) calculated from the measured Doppler frequency of RASS echoes and radar echoes into the following formula:

$$T = [(s_r - v_r)/20.0463]^2, \tag{24}$$

where *s_r* is the radial component of the wave front speed at *r*, which is measured with RASS echoes (see Fig. 3), *v_r* is the radial component of wind speed, which is measured with radar echoes received from atmospheric turbulence at *r*, *s_r - v_r = s*, and *r* is the radial vector from a radar site to the reflection point.

Figure 4 shows the temperature profile calculated by substituting the values of *s_r* in Fig. 3 and the wind speed *v_r* measured with the radar echoes from the atmospheric turbulence into Eq. (24), together with the temperature profile measured with a radiosonde at an official aerological observatory. During the measurement shown in Fig. 4, where the

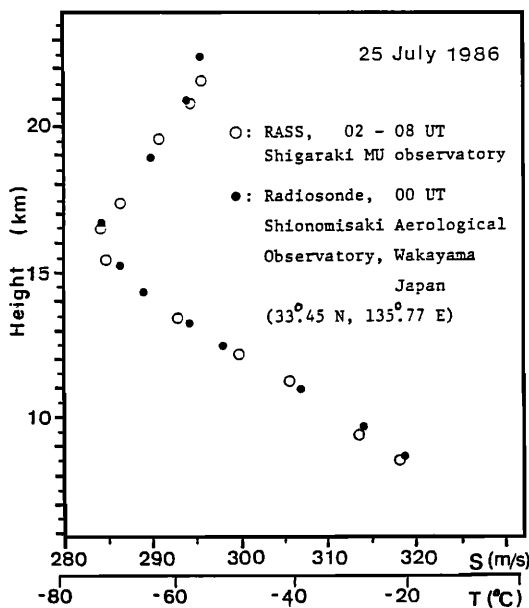


FIG. 4. Temperature profiles calculated from Doppler velocity shown in Fig. 3 and measured with a radiosonde.

maximum temperature difference is about 3 °C, the wind speed was about 20 m/s, the wind direction was unstable, the time difference between the RASS measurement and the radiosonde measurement was more than 2 h, and the distance between the RASS site and the radiosonde site was about 150 km. Where the atmosphere was measured with the RASS and the radiosonde launched by the authors at the same time and site, the temperature difference was less than 0.5 °C.

In the troposphere, a Doppler radar can easily measure the wind profiles, because the radar echoes from atmospheric turbulences are usually about 20 dB stronger than the RASS echoes. But in the stratosphere, the RASS echoes become useful for measuring the wind profiles, because the radar echoes from the turbulences are weaker than the RASS echoes there.

Now, we show a method of obtaining the atmospheric profiles of temperature and wind by using only the RASS echoes for two reflection positions P_1 and P_2 at the same height having positive but different angles of elevation, i.e., where the RASS echoes are received from P_1 and P_2 at the same height in opposite directions (see Fig. 5). In this case, it is easy to derive the following relations:

$$-\lambda \Delta f_i / 2 = s + v \cos \varphi_i \quad (i = 1, 2, \Delta f_i < 0), \quad (25)$$

where λ is the radio wavelength, Δf_i is the Doppler frequency of RASS echoes from P_i , and φ_i is the elevation angle of P_i .

Eliminating s from the above equations and solving them for v , we get

$$v = \frac{\lambda(\Delta f_1 - \Delta f_2)}{2(\cos \varphi_2 - \cos \varphi_1)} = \frac{s_1 - s_2}{\cos \varphi_1 - \cos \varphi_2}, \quad (26)$$

where s_i is the radial component of the acoustic wave front velocity at r_i .

By a similar method, we get

$$s = \frac{\lambda(\Delta f_1 \cos \varphi_2 - \Delta f_2 \cos \varphi_1)}{2(\cos \varphi_1 - \cos \varphi_2)} = \frac{s_1 \cos \varphi_2 - s_2 \cos \varphi_1}{\cos \varphi_2 - \cos \varphi_1}. \quad (27)$$

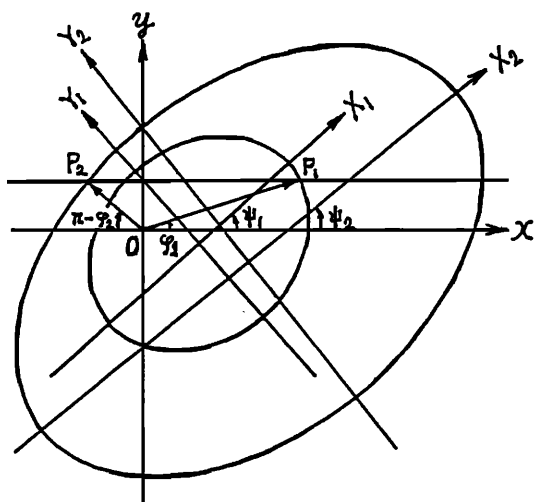


FIG. 5. Two acoustic wave front ellipses whose reflection positions P_1 and P_2 are the same height. Here, r_i is the distance between radar site O and reflection position P_i , φ_i is the elevation angle of P_i seen from O , and $i = 1, 2$.

The wind speed is calculated with Eq. (26), the acoustic speed is calculated with Eq. (27), and the temperature is calculated with Eq. (23).

Figure 6 shows the wind profile calculated with Eq. (26) and the wind profile measured with the MU radar.

IV. CONCLUSION

The acoustic wave front in the atmosphere was analyzed. In the exceptional case of no wind shear, it is approximated by a sphere whose center is underground. In the normal case where there is not only temperature gradient but also wind shear, the acoustic wave front is approximated by the ellipsoid whose principal axis tilts about 45° to the wind vector and whose center is also underground. This result is confirmed by the RASS experiment that succeeded in profiling the atmospheric temperature up to the heights of 23 km even under strong wind conditions. By utilizing the result, a conventional RASS can be converted into a system that can measure the atmospheric temperature and wind in the troposphere and stratosphere in the same way that the conventional system composed of a radiometer and a Doppler radar can. It is also noticeable that the RASS can measure the profiles automatically and continuously, unlike the radiosonde commonly used at present. But the experiments showed that further study is necessary to deduce the wind profile from the RASS echoes, especially in the stratosphere, where receiving conventional radar echoes is difficult, so they cannot be used to confirm the wind speed deduced from the RASS echoes.

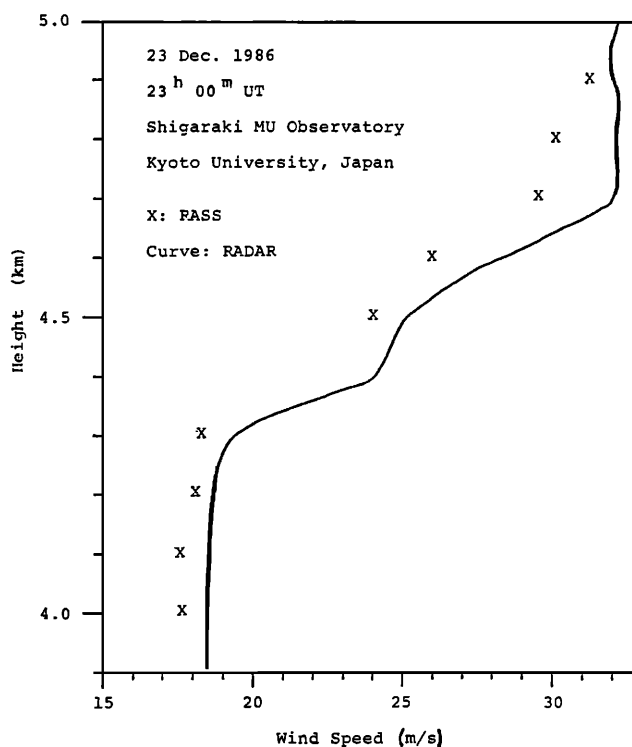


FIG. 6. Wind profiles calculated from Doppler frequencies of RASS echoes and measured with MU radar.

ACKNOWLEDGMENTS

The authors would like to express their sincere gratitude to Dr. M. Harano of the Institute for Technical Research of Ships for instructing them and supplying them with key instruments for assembling the acoustic transmitter, and also to T. Kozu of the Radio Research Laboratory for pointing out many errors in the manuscript and for giving the authors valuable comments.

APPENDIX A: PROOF OF $\dot{\varphi} = s' \cos \varphi - v' \sin \theta \cos^2 \varphi$

In Fig. A1, the acoustic wave front speed v_a in the plane of constant θ is assumed to change on the plane of $y = y_0$ as follows:

$$\begin{aligned} v_a &= s + v \sin \theta \cos \varphi, \quad \text{where } y < y_0 \\ &= (s + \delta s) + (v + \delta v) \sin \theta \cos(\varphi + \delta \varphi), \\ &\quad \text{where } y_0 < y. \end{aligned}$$

Substituting the above relations into Snell's law yields

$$\begin{aligned} \frac{s + v \sin \theta \cos \varphi}{\cos \varphi} \\ &= \frac{(s + \delta s) + (v + \delta v) \sin \theta \cos(\varphi + \delta \varphi)}{\cos(\varphi + \delta \varphi)}. \end{aligned} \quad (\text{A1})$$

Ignoring higher-order terms in (A1) yields

$$-\delta \varphi s \sin \varphi = \delta s \cos \varphi + \delta v \sin \theta \cos^2 \varphi. \quad (\text{A2})$$

Substituting (2) for $s \sin \varphi$ into (A2) yields

$$-\delta \varphi y = \delta s \cos \varphi + \delta v \sin \theta \cos^2 \varphi. \quad (\text{A3})$$

Transforming (A3), taking the limit when δs and δv approach zero, and ignoring higher-order terms yield

$$\dot{\varphi} = - \left(\frac{\partial s}{\partial y} \cos \varphi + \frac{\partial v}{\partial y} \sin \theta \cos^2 \varphi \right). \quad (\text{A4})$$

Substituting (9) and (10) into (A4) yields

$$\dot{\varphi} = s' \cos \varphi - v' \sin \theta \cos^2 \varphi. \quad (\text{A5})$$

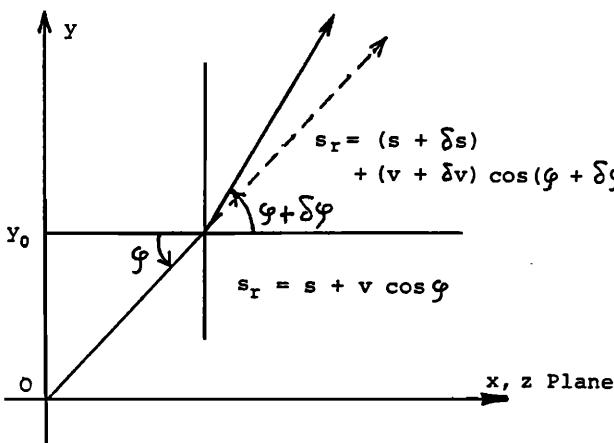


FIG. A1. Coordinate system to explain the Snell's law rotation of the plane wave front.

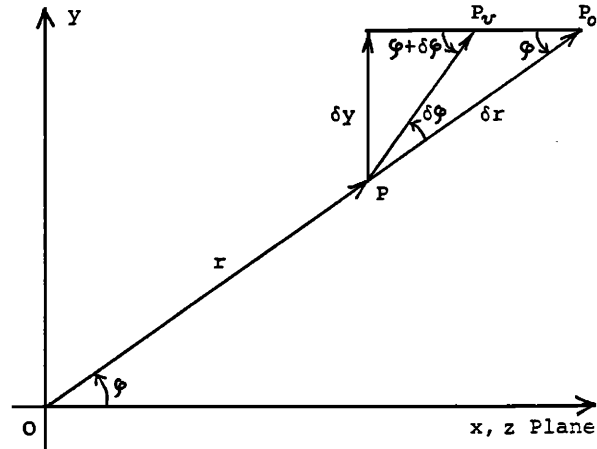


FIG. B1. Coordinate system to explain bending of the acoustic wave ray caused by wind shear on the plane of $z = 0$.

APPENDIX B: PROOF OF $\dot{\varphi} = -v' \sin \theta \sin^2 \varphi$

In Fig. B1, P , P_0 , P_v , r , φ , δr , and δt are defined in the plane of constant θ , where δy is the increment of y corresponding to the increment δt of t , and

$$\delta l = -\delta v \delta t, \quad (\text{B1})$$

$$\delta y = \delta r \sin \varphi, \quad (\text{B2})$$

$$\tan(\varphi + \delta \varphi) = \delta y / (\delta r \cos \varphi - \delta l). \quad (\text{B3})$$

Substituting (B1) and (B2) into (B3) yields

$$\tan(\varphi + \delta \varphi) = \frac{\delta r \sin \varphi}{\delta r \cos \varphi + \delta v \sin \theta \delta t}. \quad (\text{B4})$$

The left side of (B4) is approximated as follows:

$$\tan(\varphi + \delta \varphi) \doteq \frac{\tan \varphi + \delta \varphi}{1 - \tan \varphi \delta \varphi}. \quad (\text{B5})$$

Substituting (B5) into (B4) and neglecting higher-order terms yield

$$\delta r \delta \varphi (\cos \varphi + \sin^2 \varphi / \cos \varphi) = -\delta v \sin \theta \delta t \tan \varphi. \quad (\text{B6})$$

Substituting $\delta r = s \delta t$ into (B6) yields

$$\delta \varphi s \sin \varphi = -\delta v \sin \theta \sin^2 \varphi. \quad (\text{B7})$$

Substituting (2) for $s \sin \varphi$ into (B7) yields

$$\delta \varphi y = -\delta v \sin \theta \sin^2 \varphi. \quad (\text{B8})$$

Transforming (B8), taking the limit when δt approaches zero, and neglecting the higher-order terms yield

$$\dot{\varphi} = -\frac{\partial v}{\partial y} \sin \theta \sin \varphi. \quad (\text{B9})$$

Substituting (10) into (B9) yields

$$\dot{\varphi} = -v' \sin \theta \sin^2 \varphi. \quad (\text{B10})$$

¹M. S. Frankel and A. M. Peterson, "Remote temperature profiling in the lower troposphere," *Radio Sci.* **11**(3), 157-166 (1976).

²S. Fukao, T. Sato, T. Tsuda, S. Kato, K. Wakasugi, and T. Makihira, "The MU radar with an active phased array system," *Radio Sci.* **20**(6), 1155-1176 (1985).